How to cite: *Angew. Chem. Int. Ed.* **2021**, *60*, 11344–11349
International Edition: doi.org/10.1002/anie.202016196
German Edition: doi.org/10.1002/ange.202016196

VIP **Self-Replication** **Very Important Paper**

Chemical Fueling Enables Molecular Complexification of Self-Replicators**

*Shuo Yang, Gael Schaeffer, Elio Mattia, Omer Markovitch, Kai Liu, Andreas S. Hussain, Jim Ottelé, Ankush Sood, and Sijbren Otto**

Abstract: *Unravelling how the complexity of living systems can (have) emerge(d) from simple chemical reactions is one of the grand challenges in contemporary science. Evolving systems of self-replicating molecules may hold the key to this question. Here we show that, when a system of replicators is subjected to a regime where replication competes with replicator destruction, simple and fast replicators can give way to more complex and slower ones. The structurally more complex replicator was found to be functionally more proficient in the catalysis of a model reaction. These results show that chemical fueling can maintain systems of replicators out of equilibrium, populating more complex replicators that are otherwise not readily accessible. Such complexification represents an important requirement for achieving open-ended evolution as it should allow improved and ultimately also new functions to emerge.*

Introduction

Life can be considered as an emergent property of a highly complex chemical system. Establishing how chemical systems can complexify to the point that life emerges is among the grand challenges in contemporary science. In the different approaches to this question,[1–4] self-replicating systems[5–9] play an essential role. The heritability associated with self-replicating systems enables Darwinian evolution,[10,11] which has proven to be a powerful mechanism for complexification. However, in many experiments on the evolution of replicators the opposite was observed: replicators have a tendency to become smaller as smaller replicators tend to be replicated faster.[12–15] Nonetheless, complexification is essential in the transition of chemistry into biology, as the continuous invention of new functions is likely to require systems of increasing complexity.[1,2]

The transitions from non-living matter to primitive life to evolved life are associated with an increase in molecular complexity and ordering. Producing a state of local ordering is entropically costly and can only occur if it is coupled to and accompanied by a larger increase in the entropy of the surroundings. A living organism is able to reach and maintain its complex entropically disfavored and far-from-equilibrium state by coupling its internal organization to chemical processes that are producing entropy externally, like the burning of a fuel. Inspired by this mechanism, we reasoned that the chemical fueling of a process of self-replication should enable the molecular complexification of the replicator.

Chemical fueling has been utilized to achieve dissipative self-assembly,[16–23] to drive micellization-driven physical autocatalysts out of equilibrium,[24] and to create bistability in replicator networks.[25] No molecular complexification was observed in these fueled systems.

Chemically fueled replication may be implemented by creating a regime in which replicator formation competes with replicator destruction and at least one of these processes is driven by a high-energy reactant. We decided to test this important concept of fueled molecular complexification using a system of fully synthetic replicators (i.e. unconstrained by canonical biochemistry or considerations of prebiotic relevance). We previously reported a system of self-assembly driven self-replication[26–29] that could potentially be subjected to a chemically fueled replication–destruction regime. In brief, oxidation of dithiol building block **1** yields a mixture of disulfides of different ring sizes that interconvert through disulfide exchange.[30] If rings of a specific size are able to self-assemble by stacking into fibers, this stabilizes this ring and the composition will change to produce more of the very ring that assembles, resulting in self-replication (Figure 1A). Mechanically induced breakage of the fibers increases the number of ends from which the fibers grow, enabling exponential growth[27] of the replicator. We now report that chemically fueling a system in which two differently sized replicators compete for a common building block results in the population of the replicator with the highest molecular complexity,[31,32] even though the more complex replicator replicates slower than its competitor.

[*] S. Yang, Dr. G. Schaeffer, Dr. E. Mattia, Dr. O. Markovitch, Dr. K. Liu, A. S. Hussain, J. Ottelé, A. Sood, Prof. Dr. S. Otto
Centre for Systems Chemistry
Stratingh Institute, University of Groningen
Nijenborgh 4, 9747 AG Groningen (The Netherlands)
E-mail: s.otto@rug.nl
Dr. O. Markovitch
Origins Center, University of Groningen
Nijenborgh 7, 9747 AG Groningen (The Netherlands)

[**] A previous version of this manuscript has been deposited on a preprint server (https://doi.org/10.26434/chemrxiv.12162135.v1).

Supporting information and the ORCID identification number(s) for the author(s) of this article can be found under: https://doi.org/10.1002/anie.202016196.

© 2021 The Authors. Angewandte Chemie International Edition published by Wiley-VCH GmbH. This is an open access article under the terms of the Creative Commons Attribution Non-Commercial NoDerivs License, which permits use and distribution in any medium, provided the original work is properly cited, the use is non-commercial and no modifications or adaptations are made.

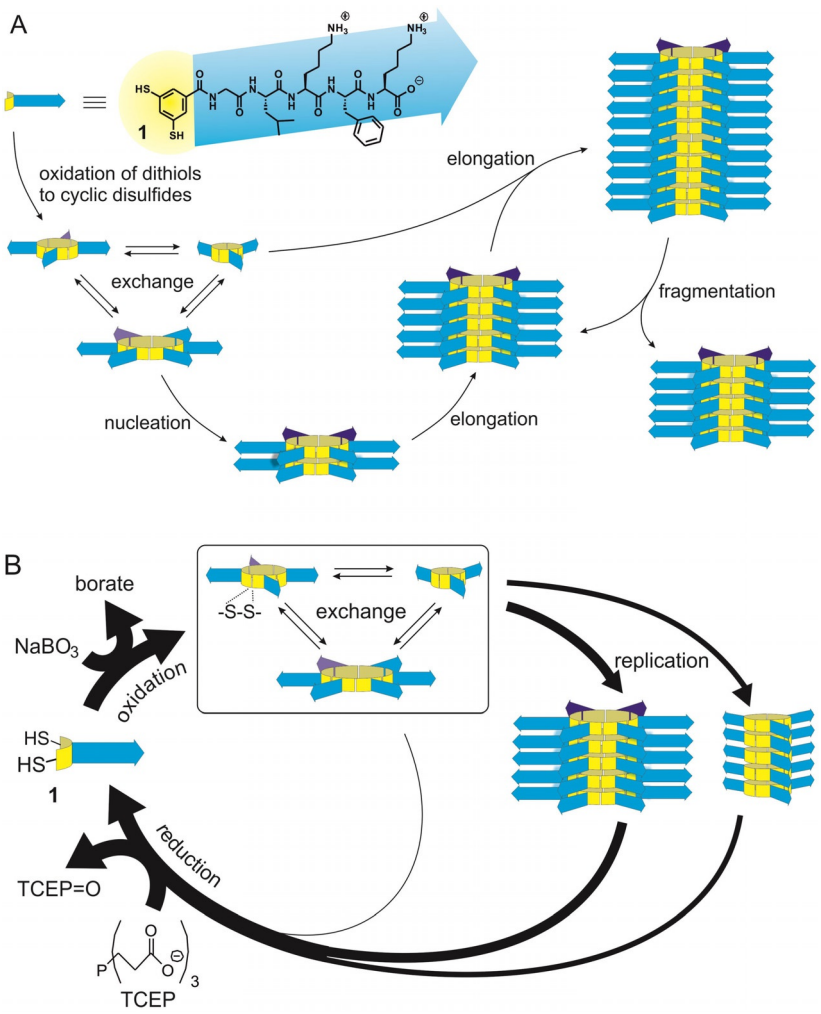

Figure 1. Schematic representation of assembly-driven self-replication in a replication–destruction regime. A) Mechanism of self-replication. Dithiol building block **1** is oxidized to give rise to a mixture of interconverting disulfides of different ring size. Slow nucleation of a stack of one particular ring size is followed by elongation of the stack. When the stack is sufficiently long to be susceptible to mechanical energy the system enters a breakage–elongation cycle leading to exponential growth of the fibers and the macrocycles from which they are constituted. B) Simplified representation of the replication–destruction regime achieved upon constant simultaneous addition of oxidant and reductant. $NaBO_3$ oxidizes the dithiol building block into a mixture of different disulfide macrocycles, from which two competing replicators can grow. TCEP reduces the disulfides in the non-assembled macrocycles as well as in the assembled replicating macrocycles back to the thiol building block. The thickness of the arrows indicates the magnitude of the fluxes (in units of **1**) through the various pathways in a kinetic model of the reaction network (SI Section S5). The flux through the short-circuiting reaction of perborate with TCEP (not shown) accounts for less than 0.1% of the total flux.

Results and Discussion

Comparing the Replication Rate and Thermodynamic Stability of Replicators 1_3 and 1_6

We discovered that building block **1**, when oxidized by oxygen from the air in the presence of guanidinium chloride, gives rise to self-replicating cyclic trimers. Their spontaneous emergence from a mixture of interconverting macrocycles was monitored over time using ultra performance liquid chromatography (UPLC) analysis (Figure 2A). Note that UPLC peak areas can be used to quantify the relative amounts of **1** in the different replicators since the molar absorptivity of a unit of **1** was found to be independent of the ring in which it resides (SI Figure S8). Analysis by transmission electron microscopy (TEM) revealed that $\mathbf{1}_3$ assembled into fibrous aggregates (Figure 2B). The autocatalytic nature of the replication process was confirmed by seeding the sample with various amounts of trimer, which was found to accelerate trimer production (Figure 2C and SI Figure S4A–C).

This system was an attractive candidate to target fueling-driven replicator complexification, as previous work has shown that building block **1**, in the absence of guanidinium chloride, gives rise to a more complex replicator, featuring larger six-membered rings ($\mathbf{1}_6$).[29] We confirmed through seeding experiments that the latter was also able to replicate in the presence of 1.5 M guanidinium chloride (Figure 2D and SI Figure S4D–F; see SI Figure S3B for data at different guanidinium chloride concentrations), albeit less efficiently than in the absence of guanidinium chloride.[29] We currently do not understand why the trimer replicator is favored in the presence of guanidinium chloride. We did investigate whether this impediment of hexamer replication was related to the known tendency of guanidinium chloride to disrupt the secondary structure of proteins. However, thioflavin T fluorescence experiments showed that guanidinium chloride diminished the extent of β-sheet formation in hexamer stacks and trimer stacks to similar extents (see SI Figure S5).

The rate of replication of $\mathbf{1}_6$ in the presence of guanidinium chloride was smaller than that of $\mathbf{1}_3$. This difference was evident from experiments in which both replicators competed for common resources in the presence of oxygen from the air (Figure 3A), where trimer replicator dominated. We also compared the rate of replication of trimers and hexamers separately by mixing pre-formed replicator with monomer **1**, immediately followed by adding perborate (the oxidant used in the fueled replication regime; see below). The trimer replicator was able to consume essentially all the monomer before oxidation was complete (whereupon replication halts), while the hexamer replicator did so only partially (SI Figure S1). Thus, the activation barrier that separates the building blocks from the replicator is higher for replicator $\mathbf{1}_6$ than for $\mathbf{1}_3$ (i.e. $\Delta G^{\ddagger}_{ox,\mathbf{1}(6)} > \Delta G^{\ddagger}_{ox,\mathbf{1}(3)}$ as shown qualitatively in Figure 4A). This difference in replication rate is most likely a result of trimer fibers being more fragile than hexamer fibers (trimer stacks are held together by maximally three β-sheets while hexamer stacks can form up to six β-sheets), leading to more fiber ends for trimers than for hexamers

 © 2021 The Authors. Angewandte Chemie International Edition published by Wiley-VCH GmbH

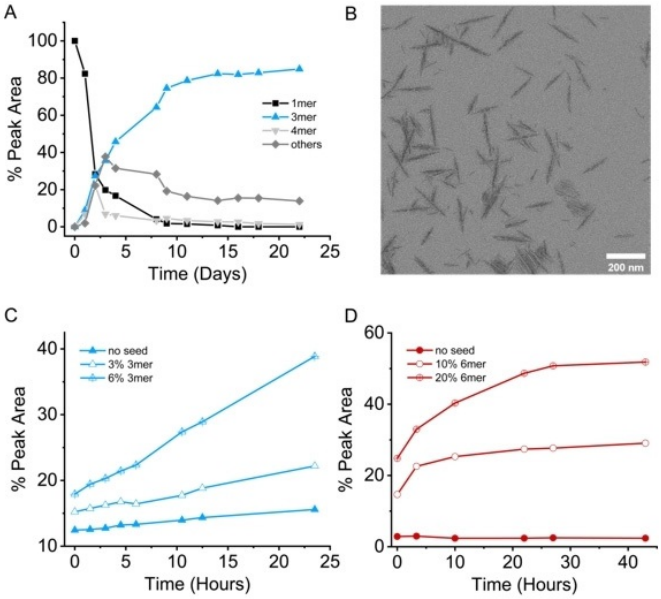

Figure 2. Self-assembly-driven self-replication of $\mathbf{1}_3$ and $\mathbf{1}_6$. A) Change in product distribution with time of a mixture made from dithiol building block **1** (0.19 mM) in borate buffer (pH 8.2) in the presence of 2.5 M guanidinium chloride. B) TEM analysis of the mixture dominated by trimers after shaking at 1200 rpm at room temperature for two weeks (scale bar = 200 nm); Change in product distribution with time of a pre-oxidized sample made from **1** (0.19 mM) in borate buffer pH 8.2 in the presence of 1.5 M guanidinium chloride in the absence and presence of various initial amounts of seeds of C) $\mathbf{1}_3$ replicator and D) $\mathbf{1}_6$ replicator. Seeding % are expressed in units of **1** relative to the total number of units of **1.** Note that the data in (C) and (D) cannot be compared directly as the experiments are started at different oxidation levels (see SI Figure S4 for details). Lines are drawn to guide the eye.

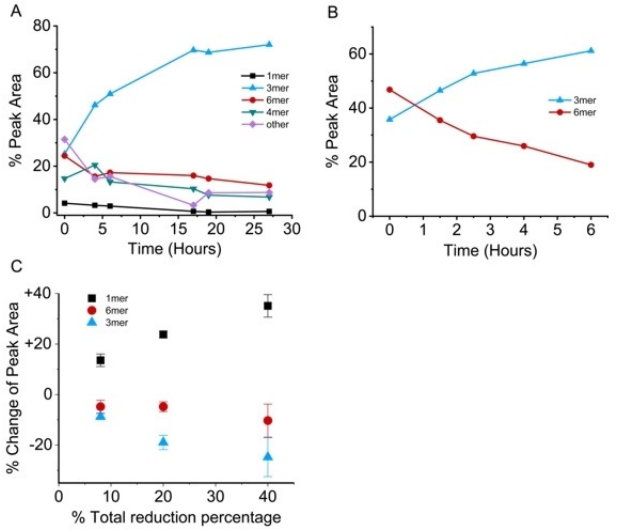

Figure 3. Comparison of the growth and/or decline of replicators $\mathbf{1}_3$ and $\mathbf{1}_6$ under different conditions. A) In a mixture of replicators $\mathbf{1}_3$ and $\mathbf{1}_6$ and non-assembled $\mathbf{1}_3$ and $\mathbf{1}_4$ macrocycles (in a 15:30:55 ratio in units of building block) $\mathbf{1}_3$ replicates faster than $\mathbf{1}_6$. The 0.50 mL sample was shaken at 1200 rpm in the presence of oxygen from the air. B) Change in product distribution with time of a mixture made from replicators $\mathbf{1}_3$ and $\mathbf{1}_6$ (approximately equimolar in units of **1**) in 1.5 M guanidinium chloride in the presence of 10 mol% dithiol **1**. Total [**1**] = 0.19 mM. C) Decrease in UPLC peak area of replicators $\mathbf{1}_3$ (blue triangles) and $\mathbf{1}_6$ (red circles) and corresponding increase in peak area of monomer **1** (black squares) upon reduction of a mixture of these replicators (0.095 mM each in units of building block **1**) to different extents by adding 8, 20, and 40 mol% TCEP (with respect to units of **1**). Error bars show the standard deviations of three independent repeats. For a statistical analysis, see SI Section S4.5. Note that hexamer-to-trimer conversion is insignificant on the time-scale of the reduction experiments. All samples were prepared in borate buffer (50 mM, pH 8.2) containing 1.5 M guanidinium chloride. Lines in (A) and (B) are drawn to guide the eye.

(evident from a fiber length analysis; see SI Figure S6). We know from previous work[27] that the rate of replication is directly proportional to the number of fiber ends.

Assessing the relative thermodynamic stabilities of both replicators proved difficult. When both replicators compete for common resources, in the absence of chemical fueling, $\mathbf{1}_3$ grows where $\mathbf{1}_6$ diminishes (Figure 3B), which would suggest that the trimer replicator is the thermodynamic product. To probe the extent to which mechanical energy influences the above outcome, control experiments were conducted in the absence of agitation. Experiments on diluted samples (to prevent assembly into long fibers for which exchange is slow[33]) confirmed the growth of trimer fibers. However, the fact that the amount of hexamer replicator only diminishes to a small extent (see SI Figure S7 and the discussion below this Figure) makes it difficult to draw a firm conclusion.

Thus, $\mathbf{1}_6$ is both a slower replicator and does not grow under conditions that would favor the formation of the thermodynamic product. Populating this replicator under conditions in which only replicator formation takes place (the experimental regime used in the vast majority of studies on self-replication) is impossible. Yet, populating $\mathbf{1}_6$ should become feasible in a regime in which both replicator formation and destruction take place, provided that the destruction of $\mathbf{1}_3$ is faster than the destruction of $\mathbf{1}_6$.

Molecular Complexification in a Chemically Fueled Replication–Destruction Cycle

A destruction reaction was readily implementable since disulfide bonds can be reduced cleanly to thiols using tricarboxyethylphosphine (TCEP; Figure 1B). We investigated the relative rate of destruction of replicators $\mathbf{1}_3$ and $\mathbf{1}_6$ in a competition experiment in which equimolar amounts of $\mathbf{1}_3$ and $\mathbf{1}_6$ were subjected to increasing concentrations of TCEP. These experiments were started in the presence of non-assembled trimer and tetramer to shorten the time to reach a stationary state. The results (Figure 3C) show that $\mathbf{1}_3$ is indeed more rapidly reduced than $\mathbf{1}_6$. Thus, the kinetic barrier for reduction of $\mathbf{1}_6$ is higher than that for the reduction of $\mathbf{1}_3$ as shown qualitatively in Figure 4A ($\Delta G^{\ddagger}_{\mathrm{rd},\mathbf{1}(6)} > \Delta G^{\ddagger}_{\mathrm{rd},\mathbf{1}(3)}$). This difference can be attributed to the fact that fibers of $\mathbf{1}_3$ are, on average, shorter than those of $\mathbf{1}_6$ (see SI Figure S6) and therefore offer more fiber ends where the reaction with TCEP takes place.[33]

An important advantage of destroying the replicator by reduction is that this reaction re-generates block **1** from which the replicator originated. This characteristic allowed us to design a protocol in which an oxidation/replication process

 © 2021 The Authors. Angewandte Chemie International Edition published by Wiley-VCH GmbH

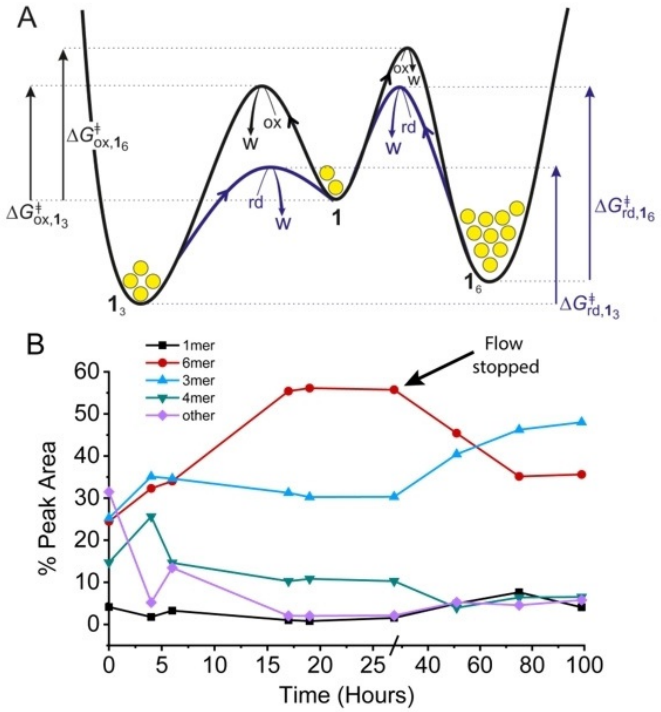

Figure 4. Population of a disfavored and slow replicator is possible in a chemically fueled replication–destruction regime. A) Potential energy landscape in which replicators $\mathbf{1}_3$ and $\mathbf{1}_6$ compete for building block **1** qualitatively showing the energy barriers for the replication (black line) and destruction (blue line) pathways. The formation of each replicator from building block **1** is coupled to the conversion of oxidant (ox) into waste (w), while the disassembly of replicators back into building block is coupled to the conversion of reducing agent (rd) into waste. It proved hard to unambiguously determine the relative thermodynamic stability of replicators $\mathbf{1}_3$ and $\mathbf{1}_6$; see SI Figure S7 and the discussion below this Figure. B) Evolution of the product distribution with time upon continuous and simultaneous addition of TCEP and $NaBO_3$ solutions to a mixture initially containing replicators $\mathbf{1}_3$ and $\mathbf{1}_6$ and non-assembled **1**, $\mathbf{1}_3$ and $\mathbf{1}_4$ (overall 0.19 mM in **1**) in 50 mM borate buffer (pH 8.2) containing 1.5 M guanidinium chloride. The black arrow indicates the moment that the addition of $NaBO_3$ was stopped. Lines are drawn to guide the eye. Five repeats of this experiment show that the behavior is qualitatively reproducible (see SI Figure S2).

takes place concurrently with TCEP-mediated replicator destruction. As oxidation mediated by oxygen from the air is relatively slow, we used sodium perborate ($NaBO_3$) as oxidant instead. Hence, the continuous additions of oxidant and reductant should result in a replication–destruction system in which the building block of the replicator is continuously recycled (Figure 1B). Note that the process of formation of the replicators from building block **1** (through the non-assembled $\mathbf{1}_3$ and $\mathbf{1}_4$ as intermediates) and their subsequent destruction back into the same building block are mediated by specific reactants (perborate and TCEP, respectively). This process is therefore not an equilibrium reaction, but rather an out-of-equilibrium chemical cycle, fueled by oxidant and reductant (see Figure 1B).

The resulting replication–destruction system contains several competing reduction and oxidation pathways. In order for the fuels (i.e. perborate and TCEP) to be coupled to the replication process it is essential that the replicators are continuously formed and broken down. Yet competing pathways exist in which perborate and TCEP mediate the formation and cleavage of non-replicating disulfide rings (mostly non-assembled $\mathbf{1}_3$ and $\mathbf{1}_4$) or in which the two fuels react directly with each other. In order to assess the relative contributions of these competing pathways we developed a kinetic model. First, we determined the majority of the involved rate constants and reaction orders experimentally, including the rates of perborate-mediated thiol oxidation and TCEP-mediated disulfide reduction, as well as the rate of the short-circuiting reaction between perborate and TCEP and the selectivity of the oxidant and reductant in producing and consuming replicator (relative to producing/consuming the non-assembling macrocycles). We also determined the kinetic order in the different reactants. Details are provided in SI Section S4 and the results are summarized in SI Table S3. We used these experimentally determined data to parameterize a kinetic model, with which we analyzed the reaction fluxes through the various competing pathways. This model was first validated and found to adequately reproduce the experimentally observed dominance of trimer replicator in the absence of fueling, shown in Figure 2A (see SI Figure S23A for the modeled behavior). The model allowed concentrations and rates of addition to be identified in which the oxidation and reduction fluxes go to a significant extent through the replicators. Furthermore, the model suggests that under the identified conditions, short-circuiting by direct reaction of perborate with TCEP occurred only to a minor extent (accounting for $<0.1\%$ of the added oxidant and reductant). The flux through reduction and re-formation (by oxidation) of non-replicating small macrocycles (0.4%) was considerably smaller than the flux through the two replicator (together 99.6%). The fluxes through the different pathways obtained from the kinetic model are shown graphically by the thickness of the arrows in Figure 1B. Details of the model are provided in SI Section S5.

We then set up replicator competition experiments under conditions of concurrent perborate and TCEP fueled replicator formation and destruction. Specifically, we prepared an agitated mixture prepared from replicators $\mathbf{1}_3$ and $\mathbf{1}_6$ and non-assembled small macrocycles (predominantly $\mathbf{1}_3$ and $\mathbf{1}_4$) in a 15:30:55 ratio in terms of building block units (total concentration of 0.19 mM in **1**). TCEP and perborate redox reagents were infused simultaneously by separate syringe pumps. In order to compensate for the higher reactivity of TCEP the rate of addition of $NaBO_3$ was double that of TCEP for the first 4 hours of the experiment. Subsequently both reagents were added at the same rate in order to maintain a steady oxidation state. By the continuous addition of 2.5 $\mu L\,h^{-1}$ of both reagent solutions (19 mM) into a 0.50 mL volume of replicator solution we achieved a nominal redox turnover time of 2 hours.

Operating the system in a fueled replication–destruction regime did indeed result in a steady state in which the slow and disfavored replicator $\mathbf{1}_6$ accounted for 60–70% of the building blocks in the mixture after 16 hours (Figure 4B and SI Figure S2). This steady state was maintained for 10 hours, corresponding to the total addition of 13 equivalents of

 © 2021 The Authors. Angewandte Chemie International Edition published by Wiley-VCH GmbH

$NaBO_3$ and 13 equivalents of TCEP. The fact that population of replicator $\mathbf{1}_6$ occurs out of equilibrium and relies upon the supply of fuel was evident from the fact that, upon stopping the supply of fuel, the system reverted back to a replicator composition that is dominated by $\mathbf{1}_3$ (Figure 4B and SI Figure S2). Note that, when fueling was halted, initially only the $NaBO_3$ supply was stopped while addition of the TCEP solution was continued for at least 10 more hours (rate of addition of 5 μL h^{-1}) to prevent the excess amount of $NaBO_3$ that is present in the stationary state (and oxygen from the atmosphere) from completely oxidizing the sample and thereby freezing the disulfide exchange. Control experiments confirmed that the build-up of TCEP oxide as a waste product does not affect the experimental outcome (see SI Figure S3A). As shown above, performing the experiment of Figure 4B without fueling with oxidant and reductant resulted in the dominance of replicator $\mathbf{1}_3$ (Figure 3A).

The experimentally observed fueling-induced increase in the amount of hexamer replicator at the expense of trimer replicator (Figure 4B and SI Figure S2) was well reproduced in the kinetic model (see SI Figure S23B).

Achieving a state of dynamic kinetic stability[1,2] (as opposed to thermodynamic equilibrium) in a system based on reversible disulfide chemistry is not trivial. The high rate of the disulfide exchange reaction offers a potentially fast competing pathway to equilibrium. Our kinetic analysis showed that disulfide exchange of non-assembled macrocycles in solution occurs on the second–minutes timescale ($k = 1.08 \pm 0.01 \times 10^4$ $M^{-1}s^{-1}$; SI Section S4.4). In the kinetic model the highest flux in the entire network is associated with the interconversion between non-assembled trimer and tetramer macrocycles (SI Table S7, reactions 5 and 6). However, as we showed previously, the rate of equilibration of disulfides slows down dramatically upon assembly of disulfides into stacks.[33] Indeed, upon stopping the supply of oxidant and reductant, the equilibration of replicator ring sizes occurs on the timescale of several days (Figure 4B). Thus, in the present system assembly is essential to allow a fueled out-of-equilibrium state to be maintained.

The Molecularly More Complex Replicator is a Better Catalyst

The results above show how chemical fueling enables the molecular complexification of the replicator, doubling its ring size. However, complexification is not an end by itself, but merely an enabler for the emergence of function. Among the most important functions in the transition from chemistry to biology is the ability to catalyze chemical reactions. In order to probe whether the complexification of the replicator structure enhances catalytic capability, we compared the abilities of both replicators to catalyze the retro-aldol reaction of substrate **2** (Figure 5A)[34] as a model chemical transformation. The data in Figure 5B show that replicator $\mathbf{1}_6$ is indeed a more proficient catalyst than its molecularly less complex competitor $\mathbf{1}_3$ and also superior to the activity of non-assembled small rings (mixture dominated by $\mathbf{1}_3$ and $\mathbf{1}_4$) and building block **1**.

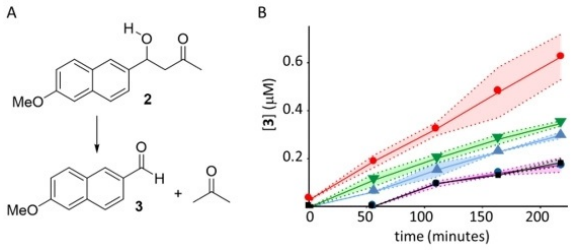

Figure 5. The more complex replicator is a more proficient catalyst. A) Retro-aldol reaction used as a model reaction to assess the catalytic proficiencies of the competing replicators. B) Kinetic data, averaged over three repeats, comparing the production of retro-aldol product **3** catalyzed by replicator $\mathbf{1}_6$ (red circles) with the effects of replicator $\mathbf{1}_3$ (blue triangles), a mixture of non-assembled $\mathbf{1}_3$ and $\mathbf{1}_4$ (green triangles), and monomer **1** (black squares). The background reaction in the absence of **1** or any of its oligomers is shown in blue circles and coincides with the data for the reaction in the presence of **1**. The concentrations of the various species were 25 μM (in units of **1**) in borate buffer (50 mM, pH 8.12) containing 1.5 M guanidinium chloride and 0.20 mM substrate **2**. Shaded areas show the standard deviation and lines are drawn to guide the eye. For a detailed mechanistic analysis of the retro-aldol reaction catalyzed by $\mathbf{1}_6$, see ref. [34]. For a repeat of the experiment at higher concentrations and temperature to give a higher conversion, see SI Figure S25.

Conclusion

The above results represent the first experimental manifestation of molecular complexification in a replicator population that is not governed by thermodynamic stability or replication efficiency alone, but rather by, what Pross has termed, its dynamic kinetic stability.[1,2] It extends beyond previous reports on dissipative systems exhibiting physical autocatalysis (autopoietic micelle formation)[24] in that molecular information is copied through specific non-covalent interactions. Furthermore, unlike in the chemically fueled replication networks reported previously in which one of the precursors of the replicator was continuously formed and broken down,[25] in the present system the fuel acts directly on replicator destruction and re-formation. Specifically, the non-assembled trimers and tetramers are high-energy states in the present system. Re-populating these from the low-energy replicator state requires the action of reductant (to convert disulfide replicators to thiol-containing building blocks and short linear oligomers) and oxidant (to convert these thiols to small non-assembled rings from which the replicators can grow spontaneously). Thus, both oxidant and reductant mediate the re-population of high-energy states and can be regarded as fuels.

Fueling enables populating molecularly more complex replicators that, in the absence of such energy supply, would not be able to compete with other faster replicators. Such molecular complexification is made possible by conducting experiments in a regime where replication as well as replicator destruction take place simultaneously. Such regime results in a replicator distribution that is governed solely by balance between the rates of replication and destruction and requires an input of (chemical) energy to continuously cycle material between building blocks and replicators. Notably, in

 © 2021 The Authors. Angewandte Chemie International Edition published by Wiley-VCH GmbH

the present system the molecular complexification of the replicator is accompanied by improved function; the more complex replicator is a better catalyst for a model retro-aldol reaction than its less complex competing replicator. Establishing the principles that enable molecular complexification of a replicator clears an important hurdle in the process of the de-novo synthesis of life, facilitates functional improvement, and, through that, may eventually enable open-ended evolution.[8,35]

Whereas fueling causes the system to increase its molecular complexity, the orthogonal parameter of informational complexity[36] does not immediately increase upon fueling. As homomeric oligomers cannot contain sequence information, increasing oligomer length has no direct effect on informational complexity. However, a higher oligomer (a hexamer in the present system) has more units that can potentially mutate than a lower oligomer (the competing trimer in the present system), and the former therefore has a superior potential for informational complexification during evolution.

Fuel-driven molecular complexification should be implementable in any system of replicators that feature, beside the replication reaction, a path that deconstructs replicators back into building blocks. In addition, this work is among the first examples of dissipative self-assembly in which more than a single bond is formed dissipatively.[37] It also shows that thiol–disulfide chemistry can be used to access out-of-equilibrium states, in which synthesis and degradation pathways through oxidation and reduction are faster than competing equilibration through thiol-mediated disulfide exchange. In the present system the ability to access a fueled out-of-equilibrium steady state relies critically on the inhibitory effect that the assembly of the disulfides into stacks has on disulfide exchange.

Acknowledgements

We gratefully acknowledge funding from the China Scholarship Council to S.Y., the NWA StartImpuls to O.M., the Netherlands Organisation for Scientific Research (Vici grant 724.012.002), the ERC (AdG 741774), and the Dutch Ministry of Education, Culture and Science (Gravitation program 024.001.035). We thank Albertas Janulevicius for help with debugging the code for the kinetic model.

Conflict of interest

The authors declare no conflict of interest.

Keywords: dissipative systems · dynamic combinatorial libraries · self-assembly · self-replication · systems chemistry

[1] A. Pross, *J. Syst. Chem.* **2011**, *2*, 1.
[2] A. Pross, *What Is Life?: How Chemistry Becomes Biology*, Oxford University Press, **2016**.
[3] J. W. Szostak, *Angew. Chem. Int. Ed.* **2017**, *56*, 11037 – 11043; *Angew. Chem.* **2017**, *129*, 11182 – 11189.
[4] K. Ruiz-Mirazo, C. Briones, A. De La Escosura, *Chem. Rev.* **2014**, *114*, 285 – 366.
[5] P. Adamski, M. Eleveld, A. Sood, Á. Kun, A. Szilágyi, T. Czárán, E. Szathmáry, S. Otto, *Nat. Rev. Chem.* **2020**, *4*, 386 – 403.
[6] V. Patzke, G. Von Kiedrowski, *ARKIVOC* **2007**, 293 – 310.
[7] G. Clixby, L. Twyman, *Org. Biomol. Chem.* **2016**, *14*, 4170 – 4184.
[8] H. Duim, S. Otto, *Beilstein J. Org. Chem.* **2017**, *13*, 1189 – 1203.
[9] T. Kosikova, D. Philp, *Chem. Soc. Rev.* **2017**, *46*, 7274 – 7305.
[10] C. Díaz Arenas, N. Lehman, *BMC Evol. Biol.* **2010**, *10*, 80.
[11] M. P. Robertson, G. F. Joyce, *Chem. Biol.* **2014**, *21*, 238 – 245.
[12] D. R. Mills, R. L. Peterson, S. Spiegelman, *Proc. Natl. Acad. Sci. USA* **1967**, *58*, 217 – 224.
[13] M. Kreysing, L. Keil, S. Lanzmich, D. Braun, *Nat. Chem.* **2015**, *7*, 203 – 208.
[14] Y. Bansho, T. Furubayashi, N. Ichihashi, T. Yomo, *Proc. Natl. Acad. Sci. USA* **2016**, *113*, 4045 – 4050.
[15] S. Matsumura, Á. Kun, M. Ryckelynck, F. Coldren, A. Szilágyi, F. Jossinet, C. Rick, P. Nghe, E. Szathmáry, A. D. Griffiths, *Science* **2016**, *354*, 1293 – 1296.
[16] M. R. Wilson, J. Solà, A. Carlone, S. M. Goldup, N. Lebrasseur, D. A. Leigh, *Nature* **2016**, *534*, 235 – 240.
[17] J. H. Van Esch, R. Klajn, S. Otto, *Chem. Soc. Rev.* **2017**, *46*, 5474 – 5475.
[18] J. Boekhoven, A. M. Brizard, K. N. K. Kowlgi, G. J. M. Koper, R. Eelkema, J. H. van Esch, *Angew. Chem. Int. Ed.* **2010**, *49*, 4825 – 4828; *Angew. Chem.* **2010**, *122*, 4935 – 4938.
[19] S. Maiti, I. Fortunati, C. Ferrante, P. Scrimin, L. J. Prins, *Nat. Chem.* **2016**, *8*, 725 – 731.
[20] G. Ragazzon, L. J. Prins, *Nat. Nanotechnol.* **2018**, *13*, 882 – 889.
[21] A. Sorrenti, J. Leira-Iglesias, A. Sato, T. M. Hermans, *Nat. Commun.* **2017**, *8*, 15899.
[22] S. Erbas-Cakmak, S. D. P. Fielden, U. Karaca, D. A. Leigh, C. T. McTernan, D. J. Tetlow, M. R. Wilson, *Science* **2017**, *358*, 340 – 343.
[23] R. D. Astumian, *Chem. Commun.* **2018**, *54*, 427 – 444.
[24] S. M. Morrow, I. Colomer, S. P. Fletcher, *Nat. Commun.* **2019**, *10*, 1011.
[25] I. Maity, N. Wagner, R. Mukherjee, D. Dev, E. Peacock-Lopez, R. Cohen-Luria, G. Ashkenasy, *Nat. Commun.* **2019**, *10*, 4636.
[26] J. W. Sadownik, E. Mattia, P. Nowak, S. Otto, *Nat. Chem.* **2016**, *8*, 264 – 269.
[27] M. Colomb-Delsuc, E. Mattia, J. W. Sadownik, S. Otto, *Nat. Commun.* **2015**, *6*, 1 – 7.
[28] J. M. A. Carnall, C. A. Waudby, A. M. Belenguer, M. C. A. Stuart, J. J.-P. Peyralans, S. Otto, *Science* **2010**, *327*, 1502 – 1506.
[29] M. Malakoutikhah, J. J. P. Peyralans, M. Colomb-Delsuc, H. Fanlo-Virgós, M. C. A. Stuart, S. Otto, *J. Am. Chem. Soc.* **2013**, *135*, 18406 – 18417.
[30] S. Otto, R. L. E. Furlan, J. K. M. Sanders, *J. Am. Chem. Soc.* **2000**, *122*, 12063 – 12064.
[31] T. Böttcher, *J. Chem. Inf. Model.* **2016**, *56*, 462 – 470.
[32] S. H. Bertz, *J. Am. Chem. Soc.* **1981**, *103*, 3599 – 3601.
[33] E. Mattia, A. Pal, G. Leonetti, S. Otto, *Synlett* **2017**, *28*, 103 – 107.
[34] J. Ottelé, A. S. Hussain, C. Mayer, S. Otto, *Nat. Catal.* **2020**, *3*, 547 – 553.
[35] K. Ruiz-Mirazo, J. Peretó, A. Moreno, *Origins Life Evol. Biospheres* **2010**, *40*, 203 – 213.
[36] T. Böttcher, *J. Mol. Evol.* **2018**, *86*, 1 – 10.
[37] M. M. Hossain, J. L. Atkinson, C. S. Hartley, *Angew. Chem. Int. Ed.* **2021**, https://doi.org/10.1002/anie.202001523.

Manuscript received: December 5, 2020
Revised manuscript received: February 9, 2021
Accepted manuscript online: March 10, 2021
Version of record online: April 8, 2021

 © 2021 The Authors. Angewandte Chemie International Edition published by Wiley-VCH GmbH